Curing kinetics study of melamine–urea–formaldehyde resin

Blaž Likozar · Romana Cerc Korošec ·
Ida Poljanšek · Primož Ogorelec · Peter Bukovec

Abstract The influence of the preconditioning at different temperatures on the cure kinetics of melamine–urea–formaldehyde resins coated on stone wool was investigated under acidic conditions using differential scanning calorimetry and thermogravimetry. The higher pre-treatment temperature was applied, to which resin-coated stone wool was exposed, the lower was the mass loss during the experiment. Kinetic model parameters were determined in two different manners, with the parameters being independent of preconditioning temperature and dependent on the latter. The apparent orders of reaction were approximately two (all of them being within the range 0.96–2.33), which would imply that cross-linking predominantly proceeds via the bimolecular reaction of either melamine or urea and formaldehyde. Nonetheless, the apparent orders of reaction decreased as a function of preconditioning temperature. The apparent activation energies varied less with preconditioning temperature, assuming values between 64.2 and 78.5 kJ mol^{-1}. The applicability of nth-order reaction kinetic models was consequently validated for two other dynamic thermal regimes.

Keywords Curing kinetics · Kinetic model · Melamine–urea–formaldehyde resin · Thermogravimetry · Differential scanning calorimetry · Composite

B. Likozar (✉)
National Institute of Chemistry, Hajdrihova 19, 1000 Ljubljana, Slovenia
e-mail: blaz.likozar@fkkt.uni-lj.si

R. C. Korošec · P. Bukovec
Faculty of Chemistry and Chemical Technology, University of Ljubljana, Aškerčeva cesta 5, 1000 Ljubljana, Slovenia
e-mail: romana.cerc-korosec@fkkt.uni-lj.si;
peter.bukovec@fkkt.uni-lj.si

I. Poljanšek
Biotechnical Faculty, University of Ljubljana, Jamnikarjeva 101, 1000 Ljubljana, Slovenia
e-mail: ida.poljansek@bf.uni-lj.si

P. Ogorelec
Melamin, kemična tovarna d.d. Kočevje, Tomšičeva cesta 9, 1330 Kocevje, Slovenia
e-mail: primoz.ogorelec@melamin.si

Introduction

Melamine–formaldehyde (MF) and melamine–urea–formaldehyde (MUF) resins are some of the most widely used adhesives for exterior and semi-exterior wood panels and for the preparation and bonding of low- and high-pressure paper laminates and overlays. Their main and significant characteristic that distinguishes them from urea–formaldehyde (UF) resins is the higher resistance to water attack and weather conditions. MF resins are expensive due to melamine and for this reason MUF resins are often used, since they have been cheapened by the addition of urea. Up to a half of melamine can be replaced by urea without seriously compromising the higher resistance to water attack and weather conditions of MF resins.

MUF resins are products which are synthesized by the step polymerization of melamine, urea and formaldehyde under alkaline or acidic conditions. Three reaction sequences must be considered, namely the formaldehyde addition to melamine or to urea (methylol formation reaction), chain growth or pre-polymer formation, and finally cross-linking or curing reaction (Fig. 1). In methylol formation reaction, nine different methylol–melamine compounds and five different methylol–urea compounds may be formed and final mixture contains both primary and

U-NH$_2$ = H$_2$N—NH$_2$ $\quad$ M-NH$_2$ = H$_2$N—N—NH$_2$
$\qquad\qquad$ || $\qquad\qquad\qquad\qquad$ | |
$\qquad\qquad$ O $\qquad\qquad\qquad\qquad$ N N
$\qquad\qquad\qquad\qquad\qquad\qquad\qquad\qquad$ ||
$\qquad\qquad\qquad\qquad\qquad\qquad\qquad\qquad$ NH$_2$

1. U-NH$_2$ + HCHO → U-NH-CH$_2$OH		methylol formation
2. U-NH-CH$_2$OH + HCHO → U-NH-(CH$_2$OH)$_2$		chain growth
3. U-NH-CH$_2$OH + U-NH$_2$ → U-NH-CH$_2$-NH-U + H$_2$O		cross-linking
4. M-NH$_2$ + HCHO → M-NH-CH$_2$OH		methylol formation
5. M-NH-CH$_2$OH + HCHO → M-NH-(CH$_2$OH)$_2$		chain growth
6. M-NH-CH$_2$OH + M-NH$_2$ → M-NH-CH$_2$-NH-M + H$_2$O		cross-linking
7. 2 U-NH-CH$_2$OH → U-NH-CH$_2$-O-CH$_2$-NH-U + H$_2$O		cross-linking

$\qquad\qquad\qquad\qquad\qquad\qquad$ ↓
$\qquad\qquad$ U-NH-CH$_2$-NH-U + HCHO

8. 2 M-NH-CH$_2$OH → M-NH-CH$_2$-O-CH$_2$-NH-M + H$_2$O		cross-linking

$\qquad\qquad\qquad\qquad\qquad\qquad$ ↓
$\qquad\qquad$ M-NH-CH$_2$-NH-M + HCHO

9. U-NH-CH$_2$OH + M-NH$_2$ → U-NH-CH$_2$-NH-M + H$_2$O		cross-linking
10. M-NH-CH$_2$OH + U-NH$_2$ → M-NH-CH$_2$-NH-U + H$_2$O		cross-linking
11. M-NH-CH$_2$OH + HOH$_2$C-NH-U → M-NH-CH$_2$-O-CH$_2$-NH-U + H$_2$O		cross-linking

$\qquad\qquad\qquad\qquad\qquad\qquad$ ↓
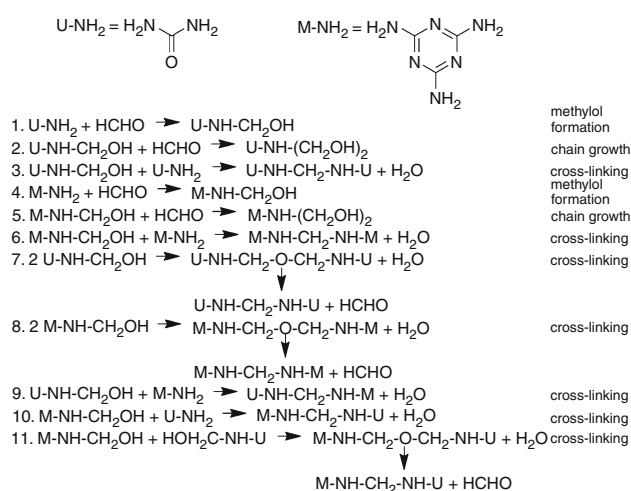$\qquad\qquad$ M-NH-CH$_2$-NH-U + HCHO

Fig. 1 The reaction scheme of melamine–urea–formaldehyde (MUF) resins

secondary methylols. In the second sequence of resin synthesis, methylol–melamine and methylol–urea condensate into methylene and methylene–ether bridges (Fig. 1). This mechanism is analogous to the one of phenol–formaldehyde resin formation, presented in our past work [1]. There are several competing reactions involved in MUF resin cross-linking process which proceed both consecutively and in parallel. The molar ratio of melamine, urea and formaldehyde, and pH conditions under which the reactions of melamine or urea with formaldehyde are carried out have a profound effect on the characteristics of resulting products.

Curing kinetics of MUF resins has not been studied extensively up to date. Higuchi et al. [2] proposed a model in which the melamine residues, incorporating a small amount of urea residues, form a three-dimensionally cross-linked network to which part of the urea residues are linked as pendants or grafts. They proposed this model as the polymeric structure of the MUF resin. Scheepers et al. [3] based Fourier transform Raman spectroscopy band assignments on a combination of literature band assignments, a study of the Raman spectra of model compounds and well characterized MF adducts and resins. Model compound studies by Jones et al. [4] suggested that >N–CH$_2$–N< bridges are less stable than widely thought unless they are in hexahydro-1,3,5-triazine ring structures. Braun and Unvericht [5] investigated possible co-condensation reactions during processing of melamine–phenol–formaldehyde (MPF) moulding materials by reacting suitable model compounds for both components (melamine and phenol) at elevated temperatures in the melt. Only recently, two quantitative kinetic modelling studies were presented by Kim et al. [6] and Cai et al. [7] both utilizing nth-order reaction kinetic models. Kim et al. [6] presented thermal

analysis study of viscoelastic properties and cross-linking reaction kinetics related activation energy of melamine-modified UF resins. On the other hand, Cai et al. [7] presented a study on the curing kinetics and viscoelastic characteristics of MUF resin in the presence of aluminium silicate nano-scale clays. Both studies, however, applied Kissinger analysis [8] obtaining the apparent activation energy as the only kinetic parameter.

Despite the fact that the kinetics or modelling of MUF curing and cross-linking were not studied up-to-date to a great extent, the cure of UF and MF was examined individually. Consequently, the curing kinetics or modelling were studied for UF themselves [9–12]; nonetheless, in some cases in combination with other reactants, such as phenol [9, 13, 14], tannin [13] and bisphenol A diglycidyl ether [15]. Analogously, different kinetic models were utilized for the curing of either neat MF [16–19] or its mixture with 8-hydroxyquinoline 5-sulphonic acid [20].

In this study, the catalyzed curing with the acidic hardener on the stone wool substrate of MUF was carried out, and the effects of preconditioning on the curing and parameters of MUF kinetics were investigated. Specifically, kinetic parameters of cross-linking process were determined, the agreement between experimental data and model predictions were estimated, the models were validated, and the sensitivity analysis was performed.

Experimental

Resin preparation

MUF resin was prepared by adding 1 mol of melamine (99 wt% pure, Aldrich) per 1 mol of urea (98 wt% pure, Sigma) under continuous mechanical stirring to reactor [containing 2.1 mol of formaldehyde (37 wt% water solution, Supelco) per mol of total amines as 40 wt% solution in water and 2.5 mol of methanol (99.9 wt% pure, provided by Melamin, kemična tovarna d.d. Kočevje) per mol of total amines]. pH was adjusted and kept at 9.3 ($\pm$0.7) with 25 wt% NaOH (98 wt% pure, Sigma-Aldrich) solution in water. Resultant mixture was heated under reflux to 90 °C within 30 min and maintained at this temperature for 200 min. During synthesis, samples were taken from reaction mixture and pH, viscosity, refraction index, the percent of dry substance and the water tolerance of resin were determined. Water tolerance was measured through the addition of 20 wt% water solution of sodium acetate (99 wt% pure, Sigma-Aldrich) to one part of resin until reaction mixture was clear. When this value reached 2.6, pH was adjusted to 9.3 ($\pm$0.7) and the excess of solvent was evaporated in order to obtain 55 ($\pm$5) wt% resin

solution. Resultant clear MUF resin was soluble in water and had the viscosity of 34 (±6) cPas at 25 °C.

Isothermal treatment of composites, high-pressure differential scanning calorimetry, thermogravimetry and scanning electron microscopy

The isothermal treatment of MUF resins deposited on stone wool at preselected temperature (i.e. from 80 to 180 °C using the interval of 10 °C) was carried out in the dryer for 20 min. The actual isothermal temperature varied for ±1 °C from the set one.

The high-pressure differential scanning calorimetry (HP DSC) measurement of thermally untreated sample was performed on the Mettler Toledo HP DSC827^e instrument in the 150 μL platinum crucible under the static air atmospheres with the pressure of 70 bar. The temperature range was from 25 to 170 °C. Heating rate was 5 °C min^{-1}. An empty pan served as a reference. The mass of sample was approximately 35 mg. Measurements with different heating rates were performed in the 150 μL aluminium crucibles under the static air atmospheres with the pressure of 70 bar. The temperature range was from 25 to 350 °C. Heating rate was 2, 5, 10, 15 and 20 °C min^{-1}. An empty pan served as a reference. The mass of sample was approximately 35 mg.

Thermogravimetry (TG) measurements were performed on the Mettler Toledo TGA/SDTA 851^e STAR^e System thermobalance under the dynamic air atmosphere (1 bar) of 100 mL min^{-1}. During isothermal measurements, furnace was heated to 140 °C at 2 °C min^{-1}, maintained at isothermal temperature for 60 min, and then heated up to 200 °C at 2 °C min^{-1}. Around 30 mg of pre-treated sample was put into the platinum crucible with the diameter of 8 mm. Baseline was subtracted for all measurements.

Results and discussion

To estimate the temperature region for the condensation reaction of MUF resin deposited on stone wool fibres, HP DSC measurement was performed (Fig. 2). Weak exothermic signal was observed in the temperature range from 25 to 45 °C, proceeding into the broad exothermic signal from this temperature up to 135 °C. It was obvious from second heating that at the beginning of measurement, weak exothermic signal was not connected with the polymerization reaction, which took place in the interval from approximately 60 to 135 °C. Figure 3, on the other hand, represents the raw data for kinetic analysis. The higher pre-treatment temperature was applied, to which resins coated stone wool was exposed, the lower was the mass loss during the experiment and also during the isothermal treatment TG segment at 140 °C. The weak exothermic
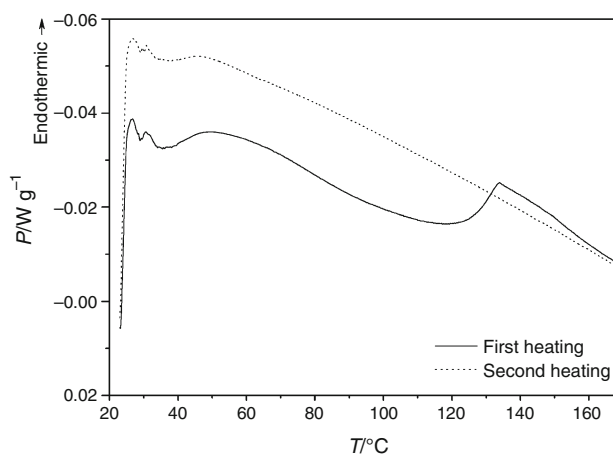

Fig. 2 HP DSC curve recorded under the pressure of 70 bar of the first and second heating experiment of thermally untreated MUF resin coated on stone wool

signal in the temperature range from 25 to 45 °C presumably derives from the formaldehyde addition to melamine or to urea (methylol formation reaction) (Fig. 1), whereas chain growth or pre-polymer formation (polymerization reaction) and finally cross-linking or curing reaction increase in extent from 60 °C upward; nonetheless, all these reactions proceed in parallel and consecutively throughout the entire temperature range, but it depends at what rate. These presumptions may be justified acknowledging thermograms in Figs. 2 and 3. If resin is completely cured (i.e. after the first heating in Fig. 2 or after the thermal treatment for 20 min at 180 °C in Fig. 3), there is practically no mass loss during subsequent heating (curve g in Fig. 3), which rules out the cross-linking reaction, as there would be noticeable mass loss due to water and formaldehyde (reaction products, Fig. 1) evaporation. Nevertheless, some formaldehyde is still trapped within cross-linked matrix and may further diffuse and react with terminal amino and methylol groups, which are much less mobile (hence the exothermic signal during the second heating in Fig. 2).

The thermal stability of samples may be determined on the basis of TG/DTG curves (Fig. 3) and the table of mass loss during dynamic curing regime (Table 1). As a rule, the thermal stability is improved with the increase of preconditioning temperature; moreover, if the temperature during preconditioning is above 150 °C, the degree of cross-linking practically reaches unity and the mass loss after preconditioning becomes negligible (<0.1 wt%). Thus, it could be considered that 150 °C is a high enough temperature to provide for relatively thermally resistant cross-linked MUF resin.

The kinetic model parameters of MUF resin cross-linking reactions had to be determined firstly and the
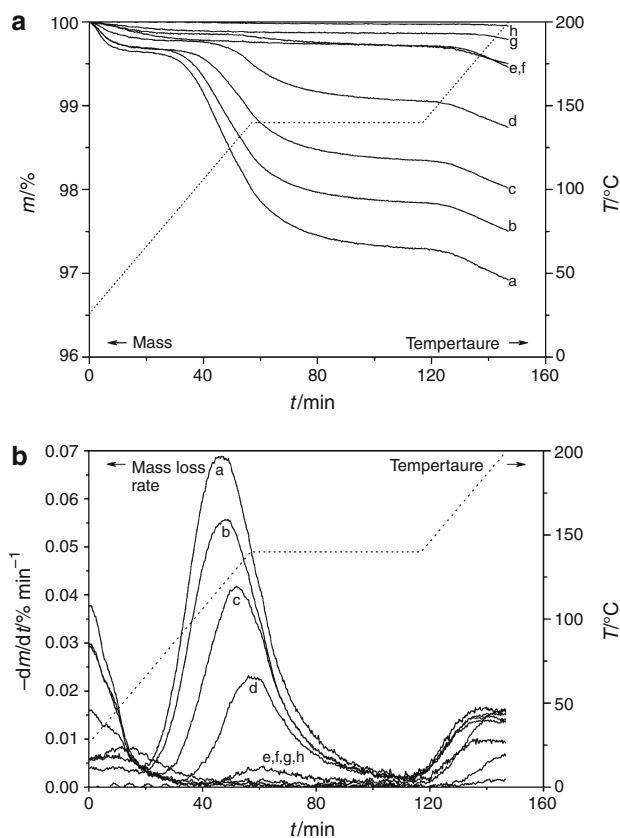
Fig. 3 Isothermal TG measurements at 140 °C (*upper figure* **a**) and corresponding DTG curves (*lower figure* **b**) for vacuum dried thermally untreated sample (*a*), samples preconditioned at 80 °C (*b*), 100 °C (*c*), 120 °C (*d*), 140 °C (*e*), 160 °C (*f*) and 180 °C (*g*) for 20 min, and bare stone wool (*h*)

Fig. 4 Algorithm used for the determination of kinetic model parameters

algorithm of their estimation is presented in Fig. 4. MUF samples were initially subjected to isothermal preconditioning for 20 min at 80–180 °C (T_i) and during this period the samples became partially cross-linked depending on preconditioning temperature. Subsequently, the samples were subjected to dynamic thermal regime (from 26 °C (T_0) to 140 °C with 2 °C min^{-1} (β); constant temperature of 140 °C between 57 min (t_1) and 117 min (t_2); from 140 to 200 °C with 2 °C min^{-1} (β); dynamic thermal regime termination after 147 min (t_3) from initiation) and during this period the experimental data for least squares curve fitting and kinetic model parameters determination was
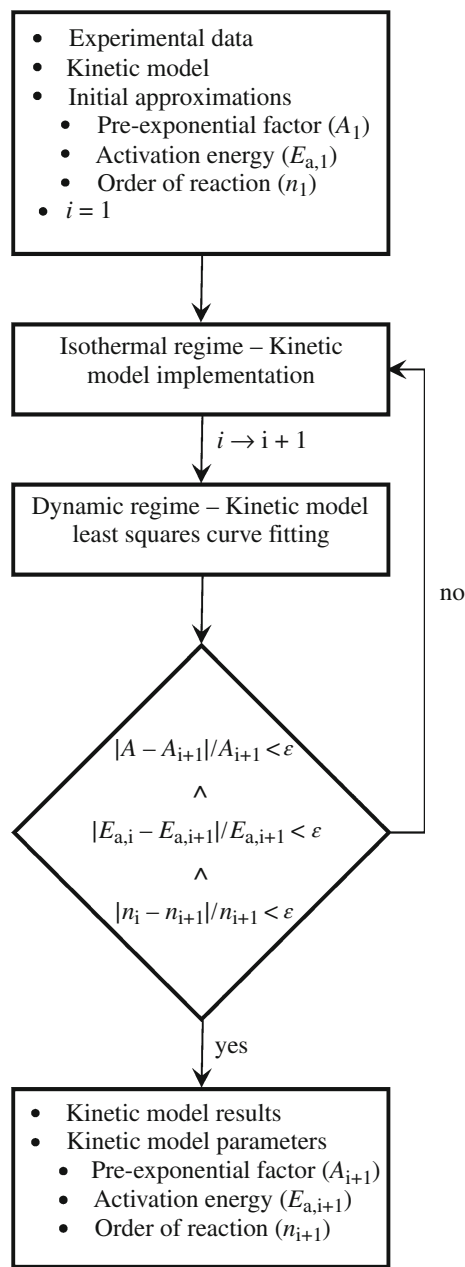
obtained. This was the experimental data referred to in first step of the algorithm (Fig. 4) and was utilized in terms of conversion, defined as

Table 1 Thermal stability of samples during dynamic curing regime following isothermal preconditioning

	Preconditioning temperature/°C											
	–	80	90	100	110	120	130	140	150	160	170	180
Mass loss/%	2.32	1.83	1.44	1.31	1.29	0.71	0.47	0.14	0.12	0.04	0.02	0.01

Dynamic regime: from 26 to 140 °C with 2 °C min^{-1}; constant temperature of 140 °C for 60 min; from 140 to 200 °C with 2 °C min^{-1}

$$a(t) = 1 - \frac{m(t) - m(\infty)}{m_{np}(0) - m_{np}(\infty)} = a_i + \frac{m(0) - m(t)}{m_{np}(0) - m_{np}(\infty)} \quad (1)$$

where a represents conversion and a_i intermediate conversion after isothermal preconditioning, respectively, m is the sample mass, m_{np} is non-preconditioned sample mass and t is time. Equation 1 implies that save for non-preconditioned sample the conversion is always higher than zero before dynamic thermal regime due to partial cross-linking during isothermal regime. The utilized nth-order reaction kinetic model [6, 7] is for isothermal regime in terms of conversion (a) and temperature (T) defined as

$$da(t)/dt = A \exp(-E_a/(RT))(1 - a(t))^n \quad (2)$$
$$dT(t)/dt = 0$$
$$a(0) = 0$$
$$T(0) = T_i$$

and for dynamic thermal regime in terms of conversion (a) and temperature (T) defined as

$$da(t)/dt = A \exp(-E_a/(RT))(1 - a(t))^n \quad (3)$$
$$dT(t)/dt = \begin{cases} \beta; & 0 \le t \le t_1 \\ 0; & t_1 < t \le t_2 \\ \beta; & t_2 < t \le t_3 \end{cases}$$
$$a(0) = a_i$$
$$T(0) = T_0$$

where A, E_a and n are the apparent pre-exponential factor, activation energy and the order of reaction, respectively. Since these kinetic model parameters were determined for the dynamic thermal regime experimental data, their initial approximations (first step of the algorithm) had to be chosen in order to simulate MUF resin cross-linking reactions during preconditioning (isothermal regime, second step of the algorithm) and determine model predicted intermediate conversion (a_i), which entered the dynamic thermal regime kinetic model through the initial condition (Eq. 3). Consequently, the initial approximations of the kinetic model parameters were corrected using least squares curve fitting to the experimental data (dynamic regime, third step of the algorithm). The values of kinetic model parameters were then compared between two consecutive iterative steps (i) (fourth step of the algorithm) and if the relative error of all kinetic model parameters between two consecutive iterative steps was less than $10^{-3}\%$ (ε), the algorithm was terminated (obtaining kinetic model results and parameters, fifth step of the algorithm), whereas otherwise the whole procedure was repeated from the second algorithm step on, until the terminal condition in ε was met (Fig. 4). The initial approximations of A, E_a and

n were taken for MF resin cross-linking reactions [21] as 57.61 kJ mol^{-1}, 8.32 × 10^6 min^{-1} and 1.12, respectively, since Kim et al. [6] and Cai et al. [7] only presented E_a values for MUF resin cross-linking reactions, however, did not present A and n values.

The kinetic model parameters were determined in two different manners, that is, the parameters being independent of preconditioning temperature (KM1) and being dependent on the latter (KM2). The variation of preconditioning temperature-independent parameters on iterative steps is presented in Fig. 5. All parameters more or less vary as compared to their initial approximations A_1, $E_{a,1}$ and n_1 during the first 20 iterations, whereas afterwards a stable set of parameters is obtained granting both the terminal condition value (ε) between consequent iterations and a Levenberg–Marquardt least squares curve fitting tolerance of 10^{-5}. Other initial approximations for A, E_a and n besides the ones mentioned above were tested in order to confirm that the determined parameter values were indeed globally the best and not only locally within a narrow parameter values range. The latter was confirmed within practical parameter range boundaries (10^{-20} s$^{-1} < A < 10^{20}$ s^{-1}, 20 kJ/mol $< E_a < 200$ kJ/mol and $0 < n < 5$). Analogous procedure was utilized for the determination of preconditioning temperature-dependent parameters.

Preconditioning temperature-independent (KM1) and preconditioning temperature-dependent (KM2) kinetic model parameters and agreement between the model and the measurements is presented in Table 2. KM1 and KM2 parameters are of the same order of magnitude; however, the agreement between the model and the measurements is much better in the case of KM2, which is expected, since the parameters were determined from individual rather than from overall fitting. The apparent orders of reaction are approximately two, both in the case of KM1 as well as
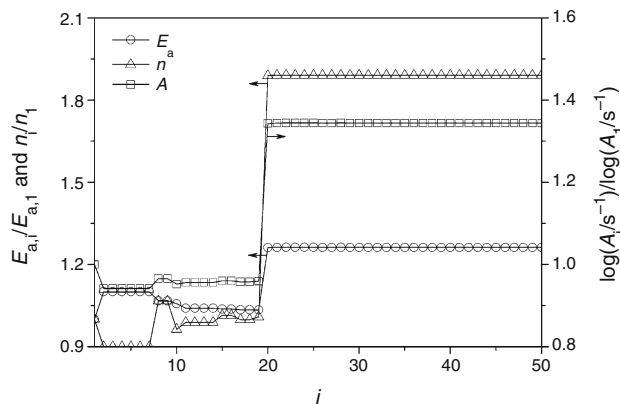
Fig. 5 The variation of preconditioning temperature-independent (KM1) kinetic model parameters with the number of algorithm iterations

Table 2 Preconditioning temperature-independent (KM1) and preconditioning temperature-dependent (KM2) kinetic model parameters and agreement between the model and the measurements presented as the sum of squares (SOS)

	Preconditioning temperature/°C											
	–	80	90	100	110	120	130	140	150	160	170	180
KM1												
$A/10^6$ s^{-1}	8.13											
E_a/kJ mol^{-1}	72.7											
n	2.12											
SOS	14.0	5.1	46.0	6.2	78.8	3.1	1.7	14.0	1.5	2.4	0.8	0.3
KM2												
$A/10^6$ s^{-1}	1.54	2.95	2.57	4.05	3.15	3.45	2.99	2.62	5.02	5.85	6.42	4.82
E_a/kJ mol^{-1}	68.8	70.1	68.4	70.7	71.8	70.2	70.7	66.7	72.7	70.2	64.2	78.5
n	1.49	2.21	2.62	2.33	1.90	2.13	1.53	1.94	1.50	1.76	1.80	0.96
SOS	2.3	2.6	5.6	4.5	4.0	2.8	2.2	0.2	0.1	0.0	0.2	0.0

Dynamic regime: from 26 to 140 °C with 2 °C min^{-1}; constant temperature of 140 °C for 60 min; from 140 to 200 °C with 2 °C min^{-1}

KM2, which would imply that cross-linking predominantly proceeds via bimolecular reaction of either melamine or urea and formaldehyde. Nonetheless, the apparent orders of reaction (KM2) decrease when plotted as a function of the preconditioning temperature. This may be explained by the fact that MUF resin cross-linking reactions generally proceed in two stages; specifically, the bimolecular reactions of either melamine or urea and formaldehyde, which is followed by the consecutive monomolecular reactions of methylene cross-link formation (Fig. 1). Both types of reactions take place simultaneously; however, methylene cross-link formation is a consecutive reaction to the mentioned bimolecular cross-link formation, and the global maximum in the rate of methylene cross-link formation reactions always follows the global maximum in the rate of reactions between either melamine or urea and formaldehyde. Since higher preconditioning temperature provides for the greater extent of the latter reactions, the reactions are shifted towards methylene cross-link formation during dynamic thermal regime, thus the transition towards lower apparent orders of reaction. The apparent order of reaction is lower in the case of MF that is 1.12–1.49 [21], which hints to predominance of methylene cross-link formation reactions. The apparent activation energies (KM2) vary less with preconditioning temperature than the orders of reaction, assuming values between 64.2 and 78.5 kJ mol^{-1}. The determined apparent activation energy of KM1 lies between minimal and maximal value of KM2 as can be observed for the determined apparent order of reaction of KM1 (between 0.96 and 2.62). This is due to the fact that kinetic parameters of KM1 provide the best fit for all utilized preconditioning temperatures and are therefore expected to reflect an average cross-linking process during dynamic thermal regime. Owing to this, the KM2 predicted conversion increases too similarly during isothermal
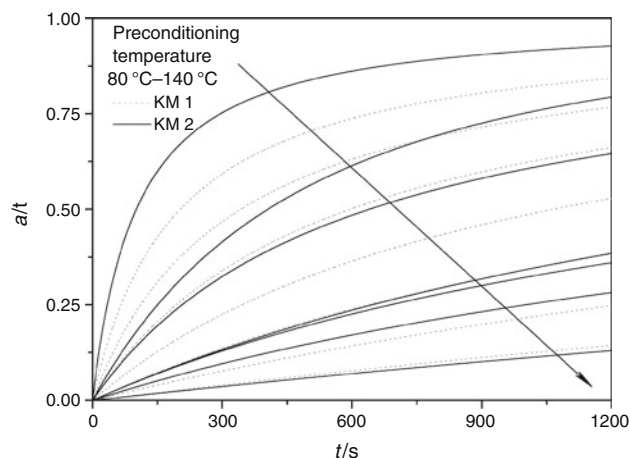
Fig. 6 The dependence of conversion on time during isothermal preconditioning as predicted by kinetic models (KM1 and KM2)

preconditioning at 110 and 120 °C (Fig. 6), but KM2 predicted conversions during dynamic thermal regime agree much better with measured data than KM1 predicted ones as can be seen from Fig. 7 and Table 2. The apparent activation energy for neat MUF resin cross-linking process is expected to be around 57.7 kJ mol^{-1} [7] which is lower than determined in this study. Nevertheless, the same authors show, that the addition of aluminium silicate nanoscale clays into MUF resin increase the apparent activation energy to 69.4 kJ mol^{-1} [7]. This apparent activation energy is practically the same as determined in this study, thus it may be deducted that the cross-linking process proceeds to a large extent according to the same mechanisms as in the case of the MUF mixture with the mentioned nano-scale clays. The minute increase in the apparent activation energies when plotted versus preconditioning temperature and an increase in the apparent pre-exponential factor may be attributed to the shifting of
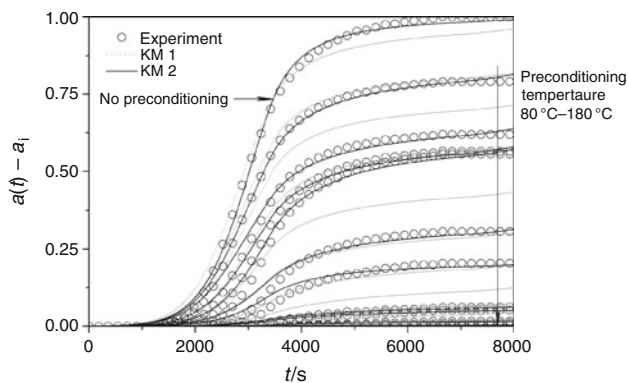
Fig. 7 The dependence of conversion on time during dynamic regime (from 26 to 140 °C with 2 °C min^{-1}, constant temperature of 140 °C for 60 min, from 140 to 200 °C with 2 °C min^{-1}) as determined from measurements and predicted by kinetic models (KM1 and KM2)

methylol cross-link formation reactions towards methylene cross-link formation reactions as well, the latter apparently having both higher apparent activation energies and pre-exponential factors, respectively; nonetheless, both kinetic parameters combined increase the apparent reaction rate constant. The order of magnitude of the apparent pre-exponential factors is the same as for MF resin cross-linking process [21] that is 10^6 s^{-1}.

Intermediate conversion after isothermal preconditioning determined from experiments and predicted by kinetic models is presented in Table 3. For the majority of pre-conditioning temperatures, as well as in overall KM2

provides much better agreement between experimental and model-predicted intermediate conversions than KM1, because of the same reasons mentioned above. Intermediate conversions increase upon choosing a higher preconditioning temperature. For 170 and 180 °C, the cross-linking is basically terminated at the end of isothermal regime as the experimental conversion is higher than 99%.

Consequently, a sensitivity analysis was performed to establish the effect of kinetic model parameters variation on intermediate conversion and the results of this analysis are presented in Table 4. KM1 parameters were differed above and below their determined values for 25%. The apparent activation energy proved to have the greatest effect on the intermediate conversion as its variation caused that the MUF resin was either practically uncross-linked after isothermal preconditioning (E_a increase for 25%) or completely cross-linked (E_a decrease for 25%) with intermediate conversion higher than 98% for all utilized preconditioning temperatures. The effect of E_a is as profound due to the apparent reaction rate being an exponential function of temperature. The effect of A is not that noticeable due to the apparent reaction rate being linearly related to it and the intermediate conversion maximally changes for approximately 22% of its original value (no preconditioning). The apparent order of reaction affects the intermediate conversion the least as the order predominantly affects the shape of the conversion curve that is its impact is the greatest when the conversions are close to unity due to the nth-order dependence of reaction rate on

Table 3 Intermediate conversion after isothermal preconditioning determined from experiments and predicted by kinetic models (KM1 and KM2)

	Preconditioning temperature/°C										
	80	90	100	110	120	130	140	150	160	170	180
a_i/% (exp.)	21.0	38.1	43.6	44.4	69.4	79.6	93.8	94.8	98.4	99.1	99.6
a_i/% (KM1)	14.4	24.8	38.3	52.9	66.2	76.7	84.3	89.5	93.0	95.2	96.7
a_i/% (KM2)	13.0	28.3	36.1	38.5	64.6	79.4	92.8	94.4	98.0	99.7	99.8

Table 4 Sensitivity analysis of intermediate conversion (a_i/%) with varying preconditioning temperature-independent (KM1) kinetic model parameters

	Preconditioning temperature/°C										
	80	90	100	110	120	130	140	150	160	170	180
$A \times 1.25$	17.3	29.1	43.6	58.2	70.7	80.2	86.9	91.3	94.2	96.1	97.3
$E_a \times 1.25$	0.0	0.1	0.2	0.4	0.8	1.6	3.0	5.5	9.5	15.6	24.0
$n \times 1.25$	13.9	23.5	35.4	48.1	59.8	69.4	77.0	82.6	86.8	89.9	92.2
$A \times 0.75$	11.2	19.9	31.9	46.0	59.8	71.5	80.5	86.8	91.0	93.9	95.8
$E_a \times 0.75$	98.3	98.9	99.3	99.5	99.7	99.8	99.8	99.9	99.9	99.9	100.0
$n \times 0.75$	14.9	26.4	41.9	59.2	74.7	85.8	92.7	96.4	98.2	99.1	99.6

conversion. As for the most applied preconditioning temperatures, the cross-linking reactions are far from being terminated after the isothermal regime, the effect of n is minimal.

The applicability of the nth-order reaction kinetic models (KM1 and KM2) was then tested for two other dynamic thermal regimes of MUF resin cross-linking process in order to validate the algorithm for the determination of kinetic model parameters (Fig. 4) for these two other regimes. Dynamic regimes were from 26 to 130 °C with 2 °C min^{-1}, constant temperature of 130 °C for 30 min, from 130 to 200 °C with 2 °C min^{-1} (dynamic thermal regime 2) and constant temperature of 25 °C for 20 min, from 25 to 200 °C with 5 °C min^{-1} (dynamic thermal regime 3). The dependence of conversion on time during two different dynamic regimes as determined from measurements and predicted by kinetic models (KM1 and KM2) is presented in Fig. 8. Once again the agreement is excellent for KM2, whereas it is not that great for KM1, as it may be seen that for the second dynamic thermal regime the conversion predicted by KM1 by far surpasses the experimental values for the preconditioning temperature of
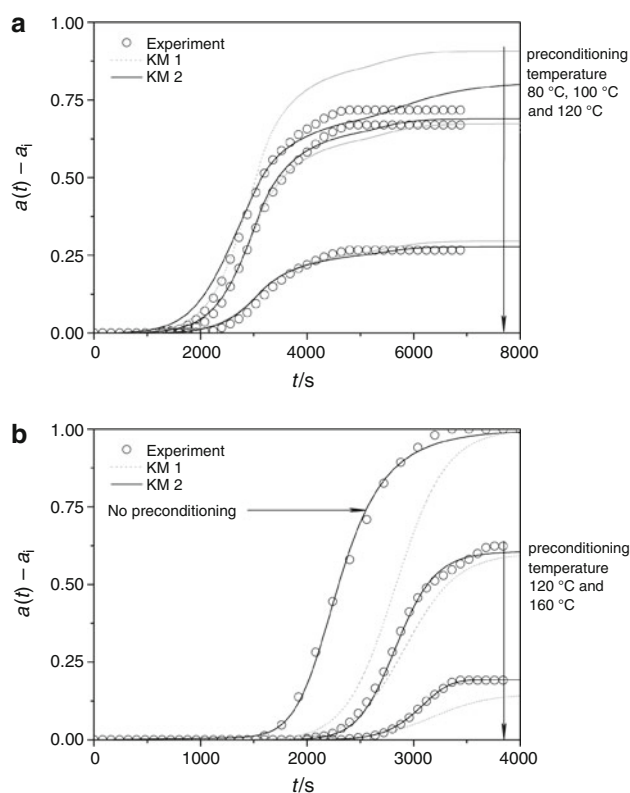

Fig. 8 The dependence of conversion on time during two different dynamic regimes [from 26 to 130 °C with 2 °C min^{-1}; constant temperature of 130 °C for 30 min; from 130 to 200 °C with 2 °C min^{-1} (*upper figure* **a**), and constant temperature of 25 °C for 20 min; from 25 to 200 °C with 5 °C min^{-1} (*lower figure* **b**)] as determined from measurements and predicted by kinetic models (KM1 and KM2)

80 °C and for the third dynamic thermal regime the conversion predicted by KM1 digresses from the experimental values after the initial agreement for all preconditioning temperatures, respectively.

The determined kinetic parameters for the second and the third dynamic thermal regime are presented in Tables 5 and 6. Here the superior agreement of KM2 with the measured values is quantitatively confirmed in terms of the sum of squares. As mentioned before, the KM2 determined

Table 5 Preconditioning temperature-independent (KM1) and preconditioning temperature-dependent (KM2) kinetic model parameters and agreement between the model and the measurements presented as the sum of squares (SOS)

	Preconditioning temperature/°C		
	80	100	120
KM1			
$A/10^7$ s^{-1}	7.78		
E_a/kJ mol^{-1}	80.9		
n	1.47		
SOS	10.9	0.4	0.2
KM2			
$A/10^7$ s^{-1}	2.94	9.52	40.83
E_a/kJ mol^{-1}	75.5	81.8	86.3
n	2.37	1.38	1.40
SOS	0.9	0.2	0.1

Dynamic regime: from 26 to 130 °C with 2 °C min^{-1}; constant temperature of 130 °C for 30 min; from 130 to 200 °C with 2 °C min^{-1}

Table 6 Preconditioning temperature-independent (KM1) and preconditioning temperature-dependent (KM2) kinetic model parameters and agreement between the model and the measurements presented as the sum of squares (SOS)

	Preconditioning temperature/°C		
	–	120	160
KM1			
$A/10^5$ s^{-1}	1.06		
E_a/kJ mol^{-1}	63.0		
n	1.29		
SOS	21.0	0.2	1.7
KM2			
$A/10^8$ s^{-1}	1.30	7.50	1.28
E_a/kJ mol^{-1}	76.6	91.5	90.7
n	2.62	1.85	1.11
SOS	0.1	0.1	0.0

Dynamic regime: constant temperature of 25 °C for 20 min; from 25 to 200 °C with 5 °C min^{-1}

apparent orders of reaction decrease with preconditioning temperature due to predominance of either methylol or methylene cross-link formation reactions. However, the apparent orders of reaction are not the same for all three regimes which may be partially contributed to the experimental error and partially to the fact that there are several competing reactions involved in the MUF resin cross-linking process that proceed both consecutively and in parallel. Thus, not only the apparent reaction order, but also the other two kinetic parameters depend on the thermal regime which differently affects the number of reactions involved in MUF resin cross-linking process. The determined kinetic model parameters are therefore an overall reflection of the predominant reaction kinetics and if these parameters were used to design a cross-linking process operation, the utilized laboratory thermal regime should be as close as possible to the one which is/will be used for the product. Nonetheless, the phenomenological nth-order reaction kinetic model is still a better alternative to the mechanistic reaction kinetic models which are seldom applicable for composite materials and are usually valid for neat resins only.

The kinetic parameters (KM2) in Tables 2, 5 and 6 depend on preconditioning temperature and the obtained dependence could be explained by the complexity of investigated process, while theoretically the correct mechanism and corresponding kinetic parameters should describe the time evolution of the system in all preconditioning conditions. Nonetheless, the cross-linking of various resins is rather complex and the reaction scheme in Fig. 1 represents only a few simplified reactions. If reaction kinetics were to be considered at a more advanced level, most of the reacting, intermediate, and produced species should be monitored over time utilizing a measuring technique such as infrared spectroscopy [1]. In contrast, differential scanning calorimetry and thermogravimetry alongside with apparent or lumped kinetics present themselves as a relatively swift and reliable alternative, but the determined kinetic parameters are system specific. However, even if a tedious mechanistic approach was to be considered, Cai et al. [7] showed that the fillers of different types and sizes also affect the cross-linking presumably due to mass transfer limitations adding even more complexity to the system. The greatest drawback, evident from Tables 2, 5 and 6 is the shifting of the apparent order of reaction between approximately 1 and 2, namely due to the simultaneous presence of monomolecular methylene and bimolecular ether cross-link formation, correspondingly. Should DSC and DTG curves exhibit at least partial separation of cross-linking peaks pertinent to individual reactions, de-convolution would present itself as a suitable option to consider these two consecutive/parallel reactions separately; nonetheless, due to complete overlapping of
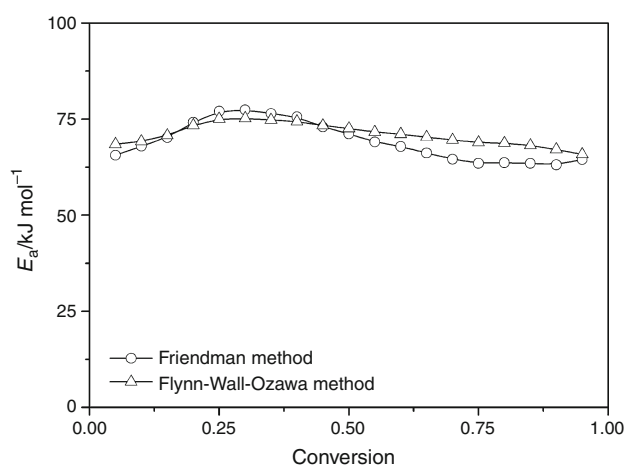

Fig. 9 Apparent activation energy as determined by Friedman [22] and Flynn–Wall–Ozawa [23, 24] methods

peaks (Figs. 2, 3), this analysis would only add to the error, which already originates from resin preparation (non-homogeneity). The preconditioning temperature-independent kinetic parameters (KM1) in Tables 2, 5 and 6 thus present the overall best set of parameters, which accurately predict the cross-linking trends, while its preconditioning temperature-dependent counterparts render an excellent fit, however, should not be ascribed to a certain underlying mechanism. Nonetheless, they are utterly useful for cross-linking process scale-up and optimization.

Lastly, it was checked if activation energy is independent of conversion degree, which was performed by using the data recorded at several heating rates and applying model-free methods, that is Friedman [22] and Flynn–Wall–Ozawa [23, 24] methods, in order to determine if E_a is independent of α and it can be supposed that the process is described by a single kinetic triplet (E_a, A and conversion function). The determined apparent activation energies are presented in Fig. 9 and it is evident that E_a indeed only slightly varies with conversion, less in the case of Flynn–Wall–Ozawa [23, 24] method utilization. The minute transition from higher to lower apparent activation energy may be interpreted through the previously mentioned consecutive/parallel reactions, which proceed simultaneously. The slightness of this transition, nonetheless, may explain the inability to separate DSC or DTG curing peak into more due to complete overlapping (very similar activation energy of the consecutive/parallel reactions pertinent to cross-linking).

Conclusions

MUF resins have great potential as the substitutes for very expensive conventional melamine–formaldehyde resins.

The higher the preconditioning temperature to which MUF resins coated stone wool was exposed the lower was the mass loss during the experiment. The obtained kinetic model parameters of KM1 (independent of preconditioning temperature) and KM2 (dependent on preconditioning temperature) were of the same order of magnitude. The agreement between model and measurements was much better in the case of KM2. The obtained apparent orders of reaction showed that cross-linking predominantly proceeded via bimolecular reaction, and that the apparent orders of reaction (and thus cross-linking mechanism) were sensitive to preconditioning temperature. The apparent activation energies varied less with preconditioning temperature and the effect of pre-exponential factor was even less noticeable. The obtained nth-order reaction kinetic model (KM2) was then tested for two other dynamic thermal regimes of MUF resin cross-linking process. The agreement between experimental data and model predictions was excellent, consequently validating the model which can successfully be utilized for different thermal regimes of cross-linking.

References

1. Poljanšek I, Likozar B, Krajnc M. Kinetics of hydroxymethyl phenols formation by in-line FTIR spectroscopy. J Appl Polym Sci. 2007;106:878–88.
2. Higuchi M, Honda T, Tajima S, Sakata I. Behavior and polymeric structures of melamine–urea–formaldehyde resin adhesives. 3. Polymeric structure deduced from the behavior of a cured resin toward acid-hydrolysis. Mokuzai Gakkaishi. 1992;38:374–81.
3. Scheepers ML, Gelan JM, Carleer RA, Adriaensens PJ, Vanderzande DJ, Kip BJ, Brandts PM. Investigation of melamine–formaldehyde cure by fourier-transform raman-spectroscopy. Vib Spectrosc. 1993;6:55–69.
4. Jones FN, Chu GB, Samaraweera U. Recent studies of self-condensation and co-condensation of melamine–formaldehyde resins—cure at low-temperatures. Prog Org Coat. 1994;24:189–208.
5. Braun D, Unvericht R. Model investigation of the co-condensation of melamine and phenol components in MPF thermoset molding materials. Angew Makromol Chem. 1995;226:183–95.
6. Kim S, Kim HJ, Kim HS, Lee YK, Yang HS. Thermal analysis study of viscoelastic properties and activation energy of melamine-modified urea–formaldehyde resins. J Adhes Sci Technol. 2006;20:803–16.
7. Cai XL, Riedl B, Wan H, Zhang SY, Wang XM. A study on the curing and viscoelastic characteristics of melamine–urea–formaldehyde resin in the presence of aluminium silicate nanoclays. Compos A. 2010;41:604–11.
8. Kissinger HE. Reaction kinetics in differential thermal analysis. Anal Chem. 1957;29:1702–6.
9. Siimer K, Christjanson P, Kaljuvee T, Pehk T, Saks I. Thermal behaviour of hydroxymethyl compounds as models for adhesive resins. J Therm Anal Calorim. 2009;97:459–66.
10. Jiang JX, Yang YL, Li C, Li JZ. Effect of three boron flame retardants on thermal curing behavior of urea formaldehyde resin. J Therm Anal Calorim. 2011;105:223–8.
11. Lu X, Pizzi A. Curing conditions effects on the characteristics of thermosetting adhesives-bonded wood joints part 2: hot postcuring improvement of UF particleboards and its temperature forecasting model. Holz Roh Werkstoff. 1998;56:393–401.
12. Carvalho Luisa MH, Costa Mario Rui PFN, Costa Carlos AV. A very simple empirical kinetic model of the acid-catalyzed cure of urea–formaldehyde resins. J Appl Polym Sci. 2006;102:5977–87.
13. Vazquez G, Lopez-Suevos F, Gonzalez-Alvarez J, Antorrena G. Curing process of phenol–urea–formaldehyde–tannin (PUFT) adhesives—kinetic studies by DSC and DMA. J Therm Anal Calorim. 2005;82:143–9.
14. He GB, Riedl B. Phenol–urea–formaldehyde cocondensed resol resins: their synthesis, curing kinetics, and network properties. J Polym Sci Pol Phys. 2003;41:1929–38.
15. Ghaemy M, Sarrafi Y, Karimi M. Curing kinetics of DGEBA/UF resin system used as laminates in impregnated decorative paper. Iran Polym J. 2010;19:661–8.
16. Winnik MA, Pinenq P, Kruger C, Zhang JX, Yaneff PV. Cross-linking vs interdiffusion rates in melamine–formaldehyde cured latex coatings: a model for waterborne automotive basecoat. J Coating Technol. 1999;71:47–60.
17. Kandelbauer A, Wuzella G, Mahendran A, Taudes I, Widsten P. Using isoconversional kinetic analysis of liquid melamine–formaldehyde resin curing to predict laminate surface properties. J Appl Polym Sci. 2009;113:2649–60.
18. Kandelbauer A, Wuzella G, Mahendran A, Taudes I, Widsten P. Model-free kinetic analysis of melamine–formaldehyde resin cure. Chem Eng Sci. 2009;152:556–65.
19. Park BD, Jeong HW. Cure kinetics of melamine–formaldehyde resin/clay/cellulose nanocomposites. J Ind Eng Chem. 2010;16:375–9.
20. Singru RN, Gurnule WB. Thermogravimetric study of 8-hydroxyquinoline 5-sulfonic acid–melamine-formaldehyde terpolymer resins-II. J Therm Anal Calorim. 2010;100:1027–36.
21. Kohl WS, Frei J, Trethewey BR. Characterization of the cure process in melamine–formaldehyde laminating resins using high-pressure differential scanning calorimetry. Tappi J. 1996;79:199–205.
22. Friedman HL. Kinetics of thermal degradation of char-forming plastics from thermogravimetry. Application to a phenolic plastic. J Polym Sci Pol Sym. 1964;6:183–95.
23. Flynn JH, Wall LA. General treatment of the thermogravimetry of polymers. J Res NBS. 1966;70A:487–523.
24. Ozawa TA. New method of analyzing thermogravimetric data. B Chem Soc Jpn. 1965;38:1881–6.